

# Ferrimagnetic resonance and low temperature transition in Ni- and Co-substituted powder magnetite

M. Y. MOHIE EL DIN

*Cairo University, Cairo, Egypt*

H. D. MERCHANT

*Continental Packaging Company, Stamford, Connecticut 06904, USA*

D. B. RUSSELL

*University of Saskatchewan, Saskatoon, Canada*

The effects of nickel and cobalt substitution on ferrimagnetic resonance in high-purity magnetite powder have been investigated. The low-temperature transition temperature and damping parameter,  $\alpha$ , are found to decrease with increasing solute additions. The linewidth,  $\Delta H$ , varies in proportion to the anisotropy field of the ferrites, narrowing with increasing nickel content but broadening with increasing cobalt content. The  $g$  factor increases with the dopant concentration, passing through a maximum around room temperature. Decreasing the deviation from stoichiometry by appropriate annealing decreases the transition temperature shift but slightly increases  $\Delta H$ ,  $g$  and  $\alpha$ .

## 1. Introduction

The low-temperature (Verwey) transition in magnetite is known to occur over a temperature range of several degrees, and to become altogether smeared out in the samples of dubious purity and deviant stoichiometry [1]. The resistivity change is one of the most conspicuous manifestations of the transition phenomenon [2]: a broadening and shifting of the transition with deviation from stoichiometry has been observed, the transition becoming unobservable by about 1% vacancy content. The localization of electrons into  $\text{Fe}^{2+}$  and  $\text{Fe}^{3+}$  states, however, still takes place as it may be observed in the Mössbauer spectrum [3-5] at 2.5% vacancy content, the effect again disappearing at about 4% vacancy level.

The impurity effects on transition in 99.99% purity  $\text{M}_x\text{Fe}_{3-x}\text{O}_4$ , where  $\text{M} = \text{Ni}, \text{Co}$  and  $x \leq 0.02$ , have been investigated by Miyahara [6] employing the magnetic susceptibility measurements. In the present study we use at least 99.9% purity components, introduce dopant up to  $x = 0.1$ , and make electron spin resonance

measurements to characterize the transition. The fact that the area under the resonance curve vanishes at the transition [7, 8] is utilized to determine the effects of nickel and cobalt substitution in  $\text{Fe}_3\text{O}_4$ .

The ferrimagnetic resonance studies on the polycrystalline ferrites are usually conducted on sintered compacts since the ferrites used in devices are quite often in that form. The powder specimen, however, may give a clearer picture of the intrinsic resonance behaviour which may be concealed by the nature of the sintered product. Consequently, in this study we have utilized the ferrite samples in the powder form.

## 2. Procedure

The samples were prepared by the oxalate method [9, 10], using the starting materials (nickel, cobalt, iron, ammonium oxalate and oxalic acid) of 99.99% purity. The reaction product was decomposed by heating in a liberal supply of air at  $600^\circ\text{C}$  for several hours, the compositions prepared being  $\text{M}_x\text{Fe}_{3-x}\text{O}_4$  ( $\text{M} = \text{Ni}, \text{Co}$ ) where

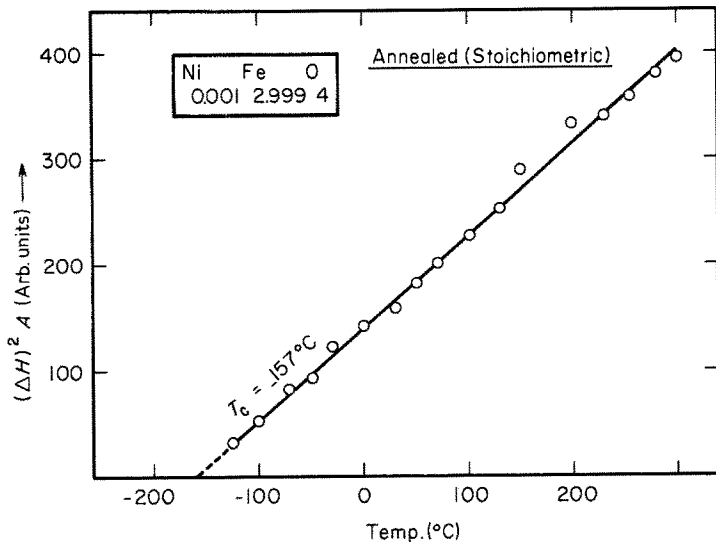


Figure 1 Effect of temperature on  $(\Delta H)^2 A$ . A typical plot.

$x = 0.001, 0.004, 0.015, 0.05$  and  $0.10$ . In order to approach as close to the stoichiometric composition as possible [11], the samples were annealed at  $1000^\circ\text{C}$  for 10 h in sealed evacuated quartz tubes and quickly quenched.

The difference between the weighed and chemically analysed compositions was not large, but the samples prior to the annealing step were found to deviate from stoichiometry. All samples before and after annealing were examined with X-ray diffraction and found to be single phase. The as-prepared powder particle size was 2 to  $5\ \mu\text{m}$  (much less than the wavelength used during the resonance measurements) and the particle shape under the microscope roughly spherical. The ferromagnetic measurements were made at  $9400\ \text{mcsec}^{-1}$  in the  $-130$  to  $300^\circ\text{C}$  temperature range, using the Varian model V-4501A electron spin resonance apparatus.

### 3. Results

The resonance curve for all specimens displayed basically the same pattern: as the temperature decreased, the linewidth increased and the amplitude decreased. The factor  $A(\Delta H)^2$ , where  $A$  is signal amplitude and  $\Delta H$  linewidth corresponds approximately to area under the resonance curve. Since the area tends to vanish at the transition temperature, the plot of  $A(\Delta H)^2$  against temperature extrapolated to  $A(\Delta H)^2 = 0$  yields the transition temperature. A typical result is shown in Fig. 1.

A certain degree of error is involved in this procedure, and due to smear in the transition temperature the error becomes larger with greater dopant

concentration. However, our main interest is determining the relative variation of the transition temperature with doping, and the extrapolation procedure gives general trends. The results are shown in Fig. 2. The temperature shift due to nickel does not seem to be significantly different from that due to cobalt. Furthermore, the shift is not simply related to the number of ferrous ions on the B sites but also becomes larger as the ionic configurations deviate from stoichiometry (unannealed specimens).

Figs. 3 and 4 show the change of linewidth with temperature. The  $\Delta H$  decreases with increasing temperature, and the annealed specimens have larger  $\Delta H$  than the corresponding unannealed ones. Furthermore, the linewidth narrows with increasing nickel content but broadens with increasing cobalt content. This effect is better seen in Fig. 5 where  $\Delta H$  at room temperature is varied with the dopant content.

Using the approximate resonance condition [12]  $\hbar\omega = g\mu H_{\text{eff}}$ , where  $\omega$  is angular frequency and  $H_{\text{eff}} = H$  for spherical particles,  $g$  values were calculated. Figs. 6 and 7 show the variation of  $g$  with temperature;  $g$  passes through a maximum around room temperature, and the peak is more pronounced for the nickel-substituted samples. The dopant effect is best illustrated in Fig. 8 where at room temperature both nickel and cobalt increase  $g$  but cobalt does so more effectively. The annealed specimens have greater  $g$  values.

Using the relation [13]  $2\alpha = \Delta H/H$ , the damping parameter  $\alpha$  was calculated. The values of  $\alpha$ , as affected by the nickel concentration, are

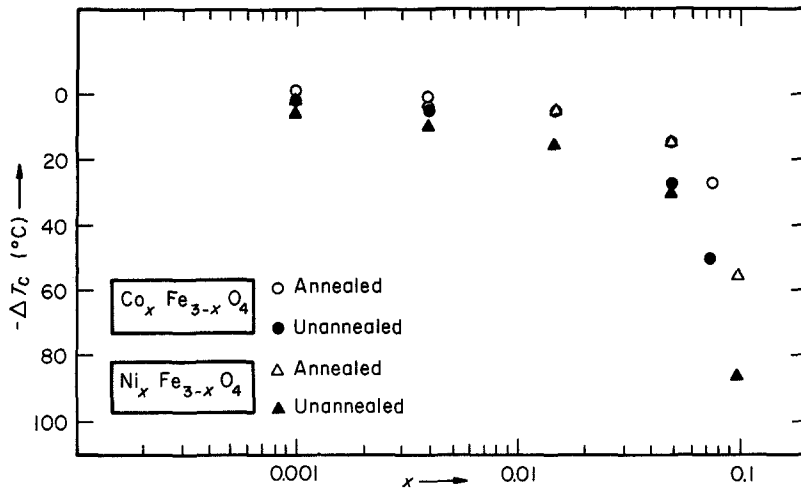


Figure 2 Depression of transition temperature due to nickel and cobalt substitution. Transition temperature ( $-153^{\circ}\text{C}$ ) for single-crystal magnetite.

shown in Fig. 9:  $\alpha$  decreases with increasing concentration and is greater for the annealed specimens.

#### 4. Discussion

The disappearance of the resonance curve of magnetite at low temperature has been observed by

several investigators, and explained by Bickford [2] as due to the existence of a large internal field at the transition temperature. In the polycrystalline solid, the internal field is dependant upon saturation magnetization, and therefore temperature, but is independent of frequency [14]. The linewidth broadening which precedes the disappearance of

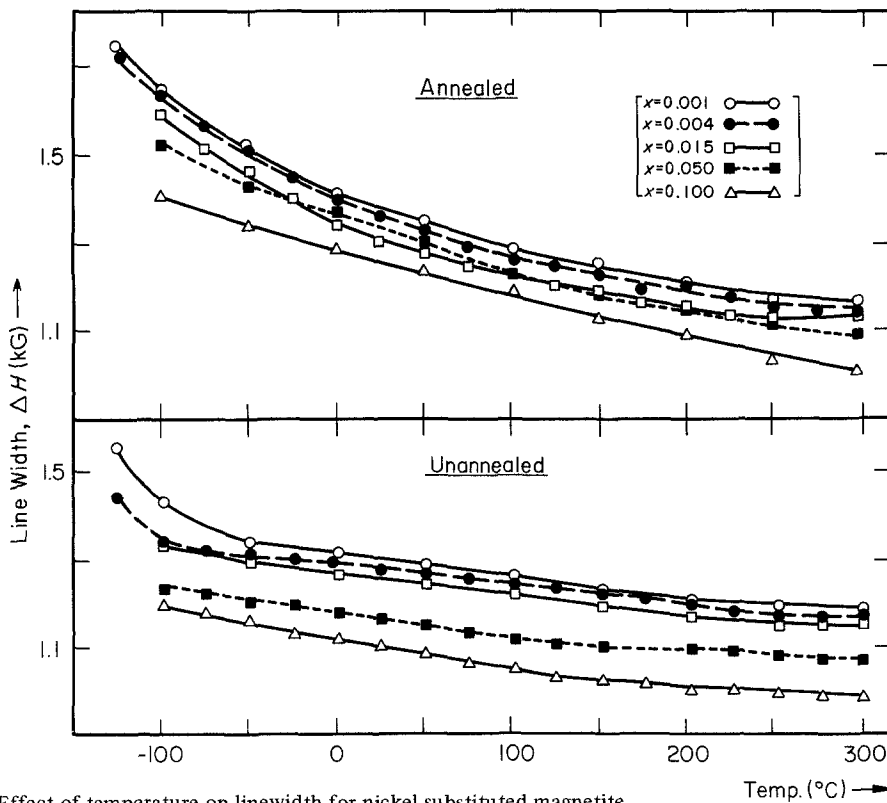


Figure 3 Effect of temperature on linewidth for nickel substituted magnetite.

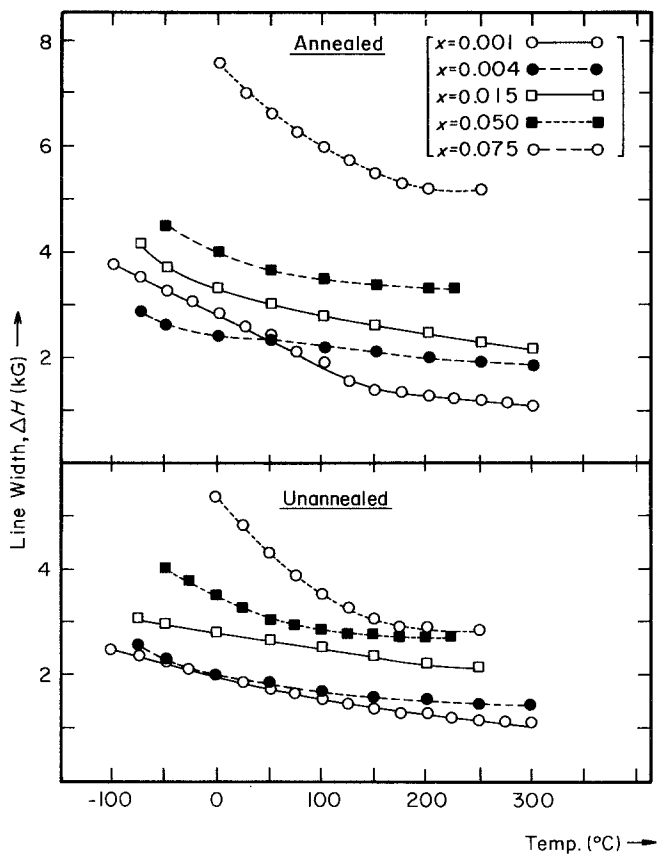


Figure 4 Effect of temperature on linewidth for cobalt substituted magnetite.

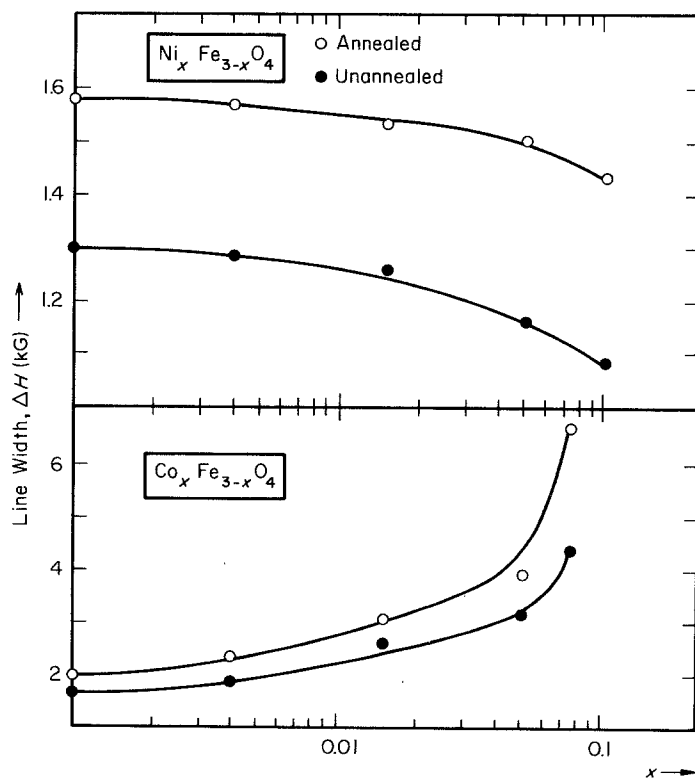


Figure 5 Effect of dopant concentration on linewidth at room temperature.

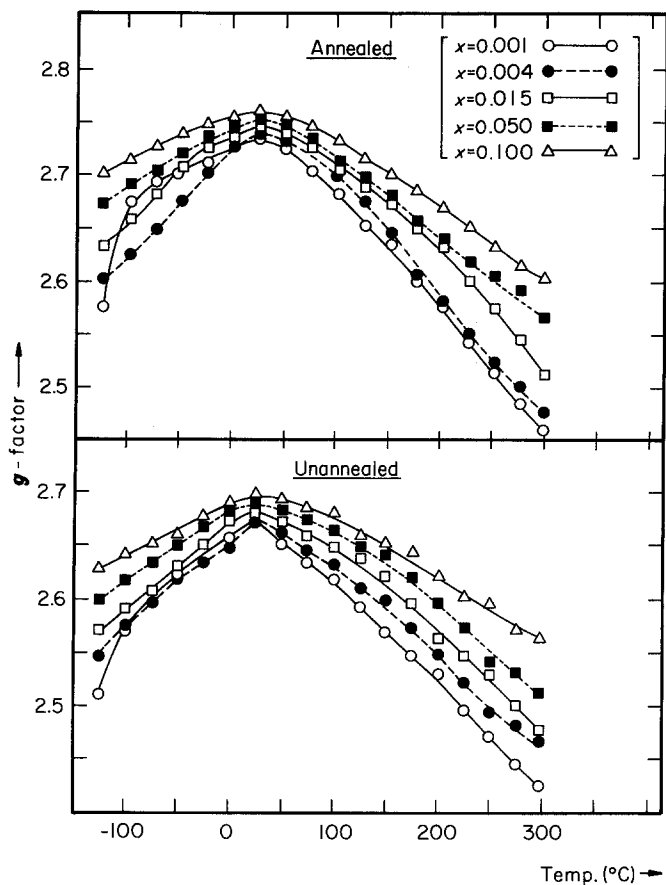


Figure 6 Effect of temperature on  $g$  factor for nickel substituted magnetite.

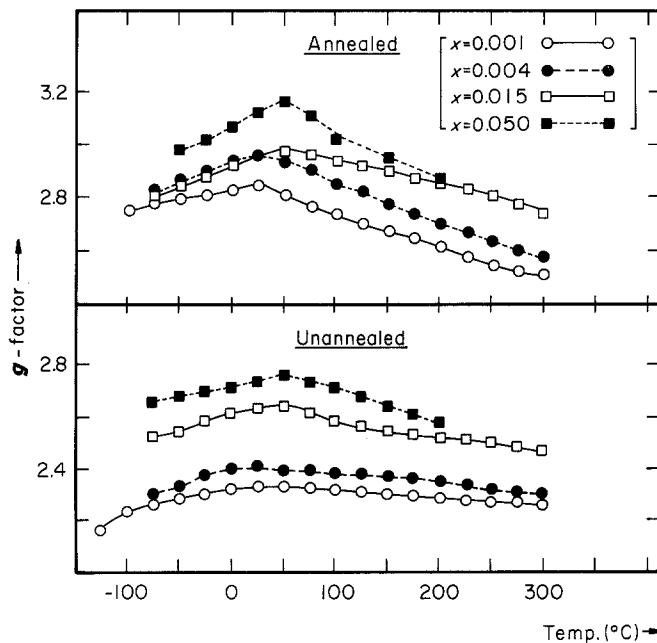


Figure 7 Effect of temperature on  $g$  factor for cobalt substituted magnetite.

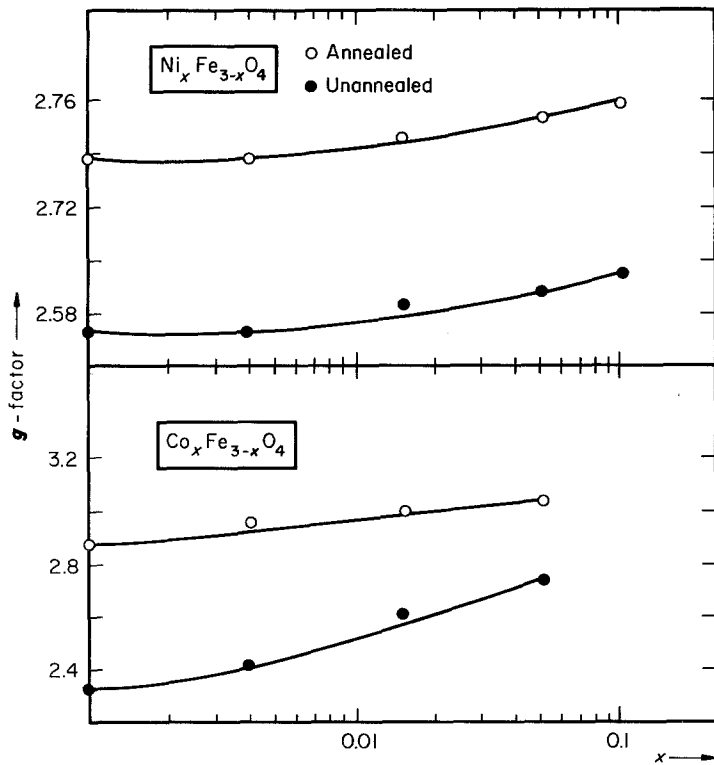


Figure 8 Effect of dopant concentration on  $g$  factor at room temperature.

resonance apparently occurs abruptly for single crystals, gradually for sintered samples, but over a range of temperatures for the powder specimens. Both the particle size distribution and polycrystallinity may explain why the absorption curve of the powder decays over such a wide temperature range.

Both deviation from the stoichiometry and ion doping result in depression of the low-temperature transition. Miyahara [6] has explained the depression due to non-stoichiometry in terms of the Wigner crystallization model [19] (increase in carrier density [20]); and due to doping in terms of the lattice distortion (impurities acting as ob-

stacles to distortion) and the double exchange model proposed by Rosenzweig [21] (impurities decreasing ordering energy without affecting exchange energy). The depression in transition temperature obtained by Miyahara is about  $5^\circ\text{C}$  for  $x = 0.002$  cobalt or nickel dopant. Our results for the corresponding dopant concentration show a depression which is approximately twice as large; furthermore, the transition temperature decreases more rapidly as either the dopant content or non-stoichiometry increases. We attribute this variance to the different purities of the samples and experimental techniques used in determining the transition temperature. It is noteworthy that as much

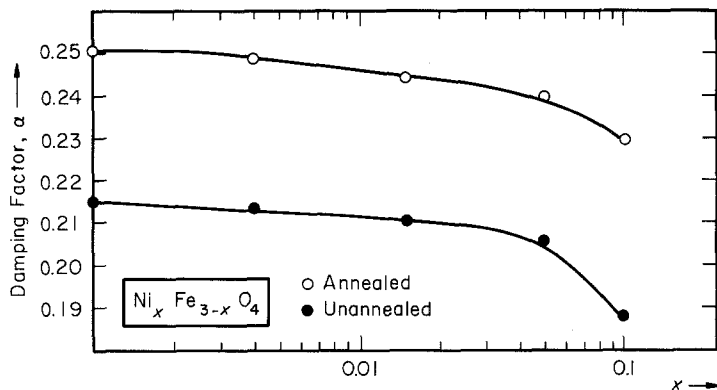


Figure 9 Effect of dopant concentration on damping factor at room temperature for nickel substituted magnetite.

as an 80°C drop in the transition temperature occurs for  $x = 0.1$ .

For the polycrystalline ferrites, the linewidth broadening was related by Harrison *et al.* [15] to the effective anisotropy constant,  $K_e$  (which equals approximately twice the magnetocrystalline anisotropy constant  $K_1$ ) [16] and the saturation magnetization,  $M_s$ : above room temperature, the linewidth depends upon  $M_s$  but below room temperature upon the anisotropy field  $2|K_1|/M_s$ . In our results,  $\Delta H$  increases rapidly with the cobalt substitution because  $2|K_1|/M_s$  is very large for cobalt ferrite as compared with that for magnetite [17]. Concurrent decrease in the ferrous ion concentration tends to narrow the linewidth, but not sufficiently to compensate for the anisotropy field effect. Furthermore,  $\Delta H$  decreases slowly with the nickel substitution because  $2|K_1|/M_s$  is smaller for nickel ferrite than for magnetite [18].

The values of  $g$  determined in this study are larger than those reported previously for the single-crystal or sintered specimen. The maximum in  $g$  near room temperature is attributed to the approach of Verwey and Curie transitions on either side of room temperature. The change in  $g$  over the low-temperature range may be correlated with the change in anisotropy energy, the lowest  $g$  occurring at the Verwey transition. Furthermore, the annealed specimens have slightly greater  $g$  than the corresponding unannealed ones. This is contrary to the prediction made by Sharma [7] that the  $g$  value of the stoichiometric and nonstoichiometric samples should coincide above the Verwey temperature. The difference in  $g$  between the annealed and the unannealed samples can be explained in terms of slight drop in the lattice parameter as the deviation from stoichiometry increases [22].

Insofar as the perturbing magnetic fields arising in ferrites with the spinel structure are proportional to the linewidth [23], increase in  $\Delta H$ , as well as decrease in the resonance field (i.e. increase in  $g$ ), would also increase the damping factor,  $\alpha$ .

Therefore, the increase in  $\alpha$  with increasing nickel content and deviation from stoichiometry, are attributed to a decrease in the ferrous ion concentration. This also explains why  $\alpha$  drops off more rapidly for the unannealed than for the annealed samples.

## References

1. E. F. WESTRUM JR and F. GRONVOLD, *J. Chem. Thermo.* **1** (1969) 543.
2. L. R. BICKFORD JR, *Phys. Rev.* **78** (1950) 449.
3. R. BAUMINGER, S. G. COHEN, A. MARINOV, S. OFTER and E. SEGAL, *ibid.* **122** (1961) 1447.
4. A. ITO, K. ONO and Y. J. ISHIKAWA, *J. Phys. Soc. Japan* **18** (1963) 1465.
5. S. K. BANERJEE, W. O'REILLY and C. E. JOHNSON, *J. Appl. Phys.* **38** (1967) 1289.
6. Y. MIYAHARA, *J. Phys. Soc. Japan* **32** (1972) 629.
7. V. N. SHARMA, *J. Appl. Phys.* **36** (1965) 1450.
8. W. A. YAGER, J. K. GALT and F. R. MERRILL, *Phys. Rev.* **99** (1955) 1203.
9. D. G. WICKHAM, M. I. T. Lab for Insulation Research, Technical Report No. 89 (1954).
10. *Idem*, *Inorg. Synthesis* **9** (1967) 152.
11. D. STERNER and H. D. MERCHANT, *J. Mater. Sci.* **8** (1973) 1823.
12. C. KITTEL, *Phys. Rev.* **73** (1947) 155.
13. N. BLOMBERGER and S. WANG, *ibid.* **93** (1954) 72.
14. T. OKAMURA, Y. TORIZAKA and Y. KOJIMA, *ibid.* **88** (1952) 1425.
15. S. E. HARRISON, H. S. BELSON and C. J. KREISSMANN, *J. Appl. Phys.* **24** (1958) 373.
16. C. J. KREISSMANN, S. E. HARRISON and H. S. BELSON, *ibid.* **29** (1958) 452.
17. P. E. TANNEWOLD, *Phys. Rev.* **99** (1955) 463.
18. R. M. BOZORTH, B. B. CETLIN, J. K. GALT, F. R. MERRITT and W. A. YAGER, *ibid.* **99** (1955) 1898.
19. E. WIGNER, *Trans. Faraday Soc.* **34** (1938) 678.
20. N. F. MOTT, *Phil. Mag.* **6** (1961) 287.
21. A. ROSENCWAIG, *Phys. Rev.* **181** (1969) 946.
22. S. J. BHATT and H. D. MERCHANT, *J. Amer. Ceram. Soc.* **52** (1969) 452.
23. A. M. CLOGSTON, H. SUHL, L. R. WALTER and P. W. ANDERSON, *Phys. Rev.* **101** (1956) 903.

Received 8 February  
and accepted 10 April 1984